VNU Journal of Science: Mathematics – Physics, Vol. 32, No. 1 (2016) 20-36

Nonlinear Stability Analysis of Imperfect Three-phase Sandwich Laminated Polymer Nanocomposite Panels Resting on Elastic Foundations in Thermal Environments

Pham Van Thu[1], Nguyen Dinh Duc[2,*]

[1]*Nha Trang University, 44 Hon Ro, Nha Trang, Khanh Hoa, Vietnam*
[2]*Vietnam National University, Hanoi, 144 Xuan Thuy, Cau Giay, Hanoi, Vietnam*

Received 10 September 2015
Revised 5 March 2016, Accepted 18 March 2016

Abstract: In this paper, the problem of nonlinear stability response of imperfect three-phase sandwich laminated polymer nanocomposite panels resting on elastic foundations in thermal environments is investigated using an analytical approach. Governing equations are derived based on classical shell theory, incorporating von Karman–Donnell type nonlinearity, initial geometrical imperfection, and Pasternak type elastic foundations. By applying the Galerkin method, an explicit expression to find the critical load and post-buckling load-deflection curves are obtained. The effects of fibres and nano-particles, material and geometrical properties, foundation stiffness, imperfection, and temperature on the buckling and post-buckling loading capacity of the three-phase sandwich laminated composite panel are analysed.

Keywords: Nonlinear stability analysis, three-phase sandwich laminated polymer nanocomposite panel, thermal environments, imperfection, elastic foundations

1. Introduction

Composite materials are used in a large number of applications; however, understanding of the structure of three-phase composite materials is limited. Díaz et al. [1] reported on analytical expressions of effective properties for three-phase piezoelectric unidirectional composites. Duc and Minh [2] presented a method to determine bending deflection of three-phase polymer composite plates consisting of reinforced glass fibres and titanium dioxide (TiO_2) particles. Lee et al. [3] investigated the silane modification of carbon nanotubes and its effects on the material properties of carbon/CNT/epoxy three-phase composites. Hoh et al. [4] carried out analytical investigations of the plastic zone crack sizes of a three-phase cylindrical composite material model. Wu et al. [5] developed a three-phase composite conductive concrete containing steel fibre, carbon fibre, and graphite for pavement deicing. Based on the Kirchhoff-Love isotropic and laminated plate theory, Wang and Zhou

*Corresponding author. Tel.: 84- 915966626
Email: ducnd@vnu.edu.vn

[6] studied the internal stress resultants of a three-phase elliptical inclusion which is bonded to an infinite matrix through an interphase layer. Chung et al. [7] presented an investigation of polymeric composite films using modified titanium dioxide TiO2 nanoparticles for organic light emitting diodes. Kalamkarov et al. [8] analysed determining the effective thermal conductivity of a composite material with periodic cylindrical inclusions of a circular cross-section arranged in a square grid. Zhang et al. [9] studied the enhancement of dielectric and electrical properties in BT/SiC/PVDF three-phase composites through microstructure tailoring. Chen et al. [10] studied the self-biased effect and dual-peak magnetoelectric effect in different three-phase magnetostrictive/piezoelectric composites. Recently, Duc and Thu [11] studied the nonlinear static analysis of a three-phase polymer composite plate under thermal and mechanical loads. Further, Duc et al. [12] presented an investigation on the nonlinear dynamic response and vibration of an imperfect laminated three-phase polymer nanocomposite panel resting on elastic foundations and subjected to hydrodynamic loads.

Sandwich laminated plates, shells and panels are basic structures used in engineering and the wider industry. These structures play an important role as the main supporting component in all kinds of structures in machinery, civil engineering, ship-building, and flight vehicle manufacturing, amongst others. The stability of composite structures is the first and foremost important condition in optimal design. Based on a fibre section analysis approach using refined material constitutive models, Hu et al. [13] developed an analysis program to analyse the moment–curvature behaviour of concrete-filled steel plate composite shear walls. Song et al. [14] investigated the sound transmission of a sandwich plate and its reduction using the stop-band concept. Mauritsson and Folkow [15] derived a hierarchy of dynamic plate equations based on the three-dimensional piezoelectric theory for a fully anisotropic piezoelectric rectangular plate. Bochkarev et al. [16] investigated the dynamic behavior of elastic coaxial cylindrical shells interacting with two flows of a perfect compressible fluid by application of the finite element method. Joshi et al. [17] proposed an analytical model for free vibration and the geometrically linear thermal buckling phenomenon of a thin rectangular isotropic plate containing a continuous line surface or internal crack located at the centre of the plate using classical plate theory. Kang et al. [18] presented the isogeometric analysis which enables the topologically complex shell structure with a single NURBS patch to be handled. Jam and Kiani [19] introduced linear buckling analysis for nanocomposite conical shells reinforced with single-walled carbon nanotubes subjected to lateral pressure. The free vibration response of functionally graded material shell structures was studied by Wali et al. [20] using an efficient 3D-shell model based on a discrete double directors shell element. Li et al. [21] presented the piecewise shear deformation theory for free vibration of composite and sandwich panels.

This paper investigated the nonlinear stability response of an imperfect sandwich laminated three-phase polymer composite panel resting on elastic foundations in thermal environments by an analytical approach. Governing equations are derived based on the classical shell theory, incorporating von Karman – Donnell type nonlinearity, initial geometrical imperfection, and Pasternak type elastic foundations. By applying the Galerkin method, the explicit expression to find critical loads and the post-buckling load-deflection curves are obtained. The effects of fibres and particles, material and geometrical properties, foundation stiffness, imperfection and temperature on the buckling and post-buckling loading capacity of the three-phase composite panel are analysed.

2. Theoretical formulation

In this paper, the algorithm that was successfully applied in [11, 12] to determine the elastic modules of three-phase composites has been used. According to this algorithm, the elastic modules of

three-phase composites are estimated using two theoretical models of the two-phase composites consecutively: nDm=Om+nD [11, 12]. This paper considers a three-phase composite reinforced with particles and unidirectional fibres, so the model of problem will be: 1Dm=Om+1D. Firstly, the modules of the effective matrix Om which is called "effective modules", are calculated. In this step, the effective matrix consists of the original matrix and added particles. It is considered to be homogeneous, isotropic, and as having two elastic modules. The next step is estimating the elastic modules for a composite material consisting of the effective matrix and unidirectional reinforced fibres.

Assuming that all the component phases (matrix, fibres and particles) are homogeneous and isotropic, we will use $E_m, E_a, E_c; \nu_m, \nu_a, \nu_c; \psi_m, \psi_a, \psi_c$ to denote Young's modulus, Poisson's ratio and the volume fraction for the matrix, fibres and particles, respectively. Following [11, 12], the modules for the effective composite can be obtained as shown below:

$$\bar{G} = G_m \frac{1-\psi_c(7-5\nu_m)H}{1+\psi_c(8-10\nu_m)H}, \quad (1)$$

$$\bar{K} = K_m \frac{1+4\psi_c G_m L(3K_m)^{-1}}{1-4\psi_c G_m L(3K_m)^{-1}}, \quad (2)$$

where

$$L = \frac{K_c - K_m}{K_c + \frac{4G_m}{3}}, H = \frac{G_m/G_c - 1}{8-10\nu_m + (7-5\nu_m)\frac{G_m}{G_c}}. \quad (3)$$

$\bar{E}, \bar{\nu}$ can be calculated from ($\bar{G}, \bar{K}$) as:

$$\bar{E} = \frac{9\bar{K}\bar{G}}{3\bar{K}+\bar{G}}, \bar{\nu} = \frac{3\bar{K}-2\bar{G}}{6\bar{K}-2\bar{G}}. \quad (4)$$

The elastic moduli for three-phase composites reinforced with unidirectional fibres are chosen to be calculated using Vanin's formulas [23], as:

$$E_{11} = \psi_a E_a + (1-\psi_a)\bar{E} + \frac{8\bar{G}\psi_a(1-\psi_a)(\nu_a - \bar{\nu})}{2-\psi_a + \bar{x}\psi_a + (1-\psi_a)(x_a-1)\frac{\bar{G}}{G_a}},$$

$$E_{22} = \left\{ \frac{\nu_{21}^2}{E_{11}} + \frac{1}{8\bar{G}} \left[\frac{2(1-\psi_a)(\bar{x}-1) + (x_a-1)(\bar{x}-1+2\psi_a)\frac{\bar{G}}{G_a}}{2-\psi_a+\bar{x}\psi_a+(1-\psi_a)(x_a-1)\frac{\bar{G}}{G_a}} + 2\frac{\bar{x}(1-\psi_a) + (1+\psi_a\bar{x})\frac{\bar{G}}{G_a}}{\bar{x}+\psi_a+(1-\psi_a)\frac{\bar{G}}{G_a}} \right] \right\}^{-1},$$

$$G_{12} = \bar{G}\frac{1+\psi_a+(1-\psi_a)\frac{\bar{G}}{G_a}}{1-\psi_a+(1+\psi_a)\frac{\bar{G}}{G_a}}, G_{23} = \bar{G}\frac{\bar{x}+\psi_a+(1-\psi_a)\frac{\bar{G}}{G_a}}{(1-\psi_a)\bar{x}+(1+\bar{x}\psi_a)\frac{\bar{G}}{G_a}}, \quad (5)$$

$$\frac{\nu_{23}}{E_{22}} = -\frac{\nu_{21}^2}{E_{11}} + \frac{1}{8\bar{G}}\left[2\frac{(1-\psi_a)\bar{x} + (1+\psi_a\bar{x})\frac{\bar{G}}{G_a}}{\bar{x}+\psi_a+(1-\psi_a)\frac{\bar{G}}{G_a}} - \frac{2(1-\psi_a)(\bar{x}-1)+(x_a-1)(\bar{x}-1+2\psi_a)\frac{\bar{G}}{G_a}}{2-\psi_a+\bar{x}\psi_a+(1-\psi_a)(x_a-1)\frac{\bar{G}}{G_a}}\right],$$

$$\nu_{21} = \bar{\nu} - \frac{(\bar{x}+1)(\bar{\nu}-\nu_a)\psi_a}{2-\psi_a+\bar{x}\psi_a+(1-\psi_a)(x_a-1)\frac{\bar{G}}{G_a}},$$

in which

$$\bar{x} = 3-4\bar{\nu}, x_a = 3-4\nu_a. \quad (6)$$

Similar to the elastic modulus, the thermal expansion coefficient of the three-phase composite materials were also identified in two steps. First, to determine the coefficient of thermal expansion of the effective matrix [22]:

$$\alpha^* = \alpha_m + (\alpha_c - \alpha_m)\frac{K_c(3K_m+4G_m)\psi_c}{K_m(3K_c+4G_m)+4(K_c-K_m)G_m\psi_c}, \quad (7)$$

in which α^* is the effective thermal expansion coefficient of the effective matrix, and α_m, α_c are the thermal expansion coefficients of the original matrix and particles, respectively. Then, determining two coefficients of thermal expansion of the three-phase composite, using formulas from [23] of Vanin, gives:

$$\alpha_1 = \alpha^* - (\alpha^* - \alpha_a)\psi_a E_1^{-1}\left[E_a + \frac{8G_a(\nu_a-\nu)(1-\psi_a)(1+\nu_a)}{2-\psi_a+\bar{x}\psi_a+(1-\psi_a)(x_a-1)\frac{\bar{G}}{G_a}}\right], \quad (8)$$

$$\alpha_2 = \alpha^* + (\alpha^* - \alpha_1)\nu_{21} - (\alpha-\alpha_a)(1+\nu_a)\frac{\nu-\nu_{21}}{\nu-\nu_a}.$$

Consider a three-phase composite panel as shown in Fig. 1. The panel is referred to a Cartesian coordinate system x, y, z, where xy is the mid-plane of the panel and z is the thickness coordinator $(-h/2 \le z \le h/2)$. The radii of curvatures, length, width, and total thickness of the panel are R, a, b and h, respectively.

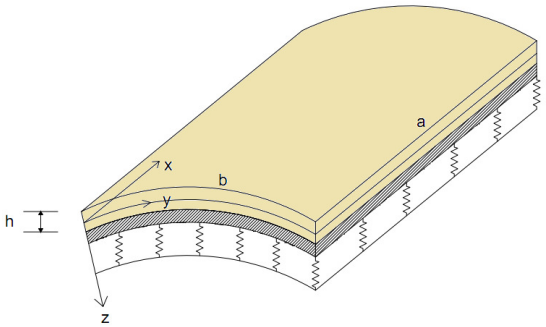

Fig. 1. Geometry and coordinate system of sandwich laminated three-phase composite panels on elastic foundations.

The three phase composite panel–foundation interaction is represented by a Pasternak model as [12, 24]:

$$q_e = k_1 w - k_2 \nabla^2 w, \quad (9)$$

where $\nabla^2 = \partial^2 / \partial x^2 + \partial^2 / \partial y^2$, and w is the deflection of the panels, k_1 is the Winkler foundation modulus, and k_2 is the shear layer foundation stiffness of the Pasternak model.

In this study, classical shell theory is used to establish the governing equations and determine the nonlinear response of three-phase composite panels [12].

$$\begin{pmatrix} \varepsilon_x \\ \varepsilon_y \\ \gamma_{xy} \end{pmatrix} = \begin{pmatrix} \varepsilon_x^0 \\ \varepsilon_y^0 \\ \gamma_{xy}^0 \end{pmatrix} + z \begin{pmatrix} k_x \\ k_y \\ 2k_{xy} \end{pmatrix}, \quad (10)$$

where

$$\begin{pmatrix} \varepsilon_x^0 \\ \varepsilon_y^0 \\ \gamma_{xy}^0 \end{pmatrix} = \begin{pmatrix} u_{,x} + w_{,x}^2 / 2 \\ v_{,y} + w_{,y}^2 / 2 - \mathrm{w} / R \\ u_{,y} + v_{,x} + w_{,x} w_{,y} \end{pmatrix}, \begin{pmatrix} k_x \\ k_y \\ k_{xy} \end{pmatrix} = \begin{pmatrix} -w_{,xx} \\ -w_{,yy} \\ -2w_{,xy} \end{pmatrix}, \quad (11)$$

in which u, v are the displacement components along the x, y directions, respectively.

Hooke's law for a laminated composite panel is defined as:

$$\begin{pmatrix} \sigma_x \\ \sigma_y \\ \sigma_{xy} \end{pmatrix}_k = \begin{pmatrix} Q_{11}^{'} & Q_{12}^{'} & Q_{16}^{'} \\ Q_{12}^{'} & Q_{22}^{'} & Q_{26}^{'} \\ Q_{16}^{'} & Q_{26}^{'} & Q_{66}^{'} \end{pmatrix}_k \begin{pmatrix} \varepsilon_x - \alpha_1 \Delta T \\ \varepsilon_y - \alpha_2 \Delta T \\ \gamma_{xy} \end{pmatrix}_k, \quad (12)$$

with

$$Q_{11} = \frac{E_1}{1 - \frac{E_2}{E_1} \nu_{12}^2} = \frac{E_1}{1 - \nu_{12}\nu_{21}}, \; Q_{22} = \frac{E_2}{1 - \frac{E_2}{E_1} \nu_{12}^2} = \frac{E_2}{E_1} Q_{11},$$

$$Q_{12} = \frac{E_1}{1 - \frac{E_2}{E_1} \nu_{12}^2} = \frac{\nu_{12}}{Q_{22}}, \; Q_{66} = G_{12}, \quad (13)$$

in which k is the number of layers and

$$\begin{aligned}
Q_{11}^{'} &= Q_{11} c\cos^4\theta + Q_{22} \sin^4\theta + 2(Q_{12} + 2Q_{66}) \sin^2\theta \cos^2\theta, \\
Q_{12}^{'} &= Q_{12} (c\cos^4\theta + \sin^4\theta) + (Q_{11} + Q_{22} - 4Q_{66}) \sin^2\theta \cos^2\theta, \\
Q_{16}^{'} &= (Q_{12} - Q_{22} + 2Q_{66}) \sin^3\theta c\cos\theta + (Q_{11} - Q_{12} - 2Q_{66}) \sin\theta c\cos^3\theta, \quad (14) \\
Q_{22}^{'} &= Q_{11} \sin^4\theta + Q_{22} c\cos^4\theta + 2(Q_{12} + 2Q_{66}) \sin^2\theta \cos^2\theta, \\
Q_{26}^{'} &= (Q_{11} - Q_{12} - 2Q_{66}) \sin^3\theta c\cos\theta + (Q_{12} - Q_{22} + 2Q_{66}) \sin\theta c\cos^3\theta, \\
Q_{66}^{'} &= Q_{66} (\sin^4\theta + c\cos^4\theta) + \left[Q_{11} + Q_{22} - 2(Q_{12} + Q_{66}) \right] \sin^2\theta c\cos^2\theta,
\end{aligned}$$

where θ is the angle between the fibre direction and the coordinate system. The force and moment resultants of the sandwich laminated composite panels are determined by:

$$N_i = \sum_{k=1}^{n} \int_{h_{k-1}}^{h_k} [\sigma_i]_k \, dz, i = x, y, xy,$$
$$M_i = \sum_{k=1}^{n} \int_{h_{k-1}}^{h_k} z[\sigma_i]_k \, dz, i = x, y, xy. \quad (15)$$

Substitution of Eq. (10) and Eq. (12) into Eq. (15), gives the constitutive relations as:

$$\left(N_x, N_y, N_{xy}\right) = (A_{11}, A_{12}, A_{16})\varepsilon_x^0 + (A_{12}, A_{22}, A_{26})\varepsilon_y^0 + (A_{16}, A_{26}, A_{66})\gamma_{xy}^0$$
$$+(B_{11}, B_{12}, B_{16})k_x + (B_{12}, B_{22}, B_{26})k_y + (B_{16}, B_{26}, B_{66})k_{xy} - \Delta T[\alpha_1(A_{11}, A_{12}, A_{16}) \quad (16a)$$
$$+\alpha_2(A_{12}, A_{22}, A_{26})],$$
$$\left(M_x, M_y, M_{xy}\right) = (B_{11}, B_{12}, B_{16})\varepsilon_x^0 + (B_{12}, B_{22}, B_{26})\varepsilon_y^0 + (B_{16}, B_{26}, B_{66})\gamma_{xy}^0$$
$$+(D_{11}, D_{12}, D_{16})k_x + (D_{12}, D_{22}, D_{26})k_y + (D_{16}, D_{26}, D_{66})k_{xy} - \Delta T[\alpha_1(B_{11}, B_{12}, B_{16}) \quad (16b)$$
$$+\alpha_2(B_{12}, B_{22}, B_{26})],$$

where

$$A_{ij} = \sum_{k=1}^{n} (Q_{ij}^{'})_k (h_k - h_{k-1}), i, j = 1, 2, 6,$$
$$B_{ij} = \frac{1}{2}\sum_{k=1}^{n} (Q_{ij}^{'})_k (h_k^2 - h_{k-1}^2), i, j = 1, 2, 6, \quad (17)$$
$$D_{ij} = \frac{1}{3}\sum_{k=1}^{n} (Q_{ij}^{'})_k (h_k^3 - h_{k-1}^3), i, j = 1, 2, 6.$$

The nonlinear equilibrium equations of the composite panels based on classical shell theory are given by:

$$N_{x,x} + N_{xy,y} = 0, \quad (18a)$$
$$N_{xy,x} + N_{y,y} = 0, \quad (18b)$$
$$M_{x,xx} + 2M_{xy,xy} + M_{y,yy} + N_x w_{,xx} + 2N_{xy} w_{,xy} + N_y w_{,yy} + q - k_1 \mathrm{w} + k_2 \nabla^2 \mathrm{w} + \frac{N_y}{R} = 0. \quad (18c)$$

Calculated from Eq. (16a), we have:

$$\varepsilon_x^0 = A_{11}^* N_x + A_{12}^* N_y + A_{16}^* N_{xy} - B_{11}^* k_x - B_{12}^* k_y - B_{16}^* k_{xy} + \Delta T(D_{11}^* \alpha_1 + D_{12}^* \alpha_2),$$
$$\varepsilon_y^0 = A_{12}^* N_x + A_{22}^* N_y + A_{26}^* N_{xy} - B_{21}^* k_x - B_{22}^* k_y - B_{26}^* k_{xy} + \Delta T(D_{21}^* \alpha_1 + D_{22}^* \alpha_2), \quad (19)$$
$$\gamma_{xy}^0 = A_{16}^* N_x + A_{26}^* N_y + A_{66}^* N_{xy} - B_{61}^* k_x - B_{62}^* k_y - B_{66}^* k_{xy} + \Delta T(D_{16}^* \alpha_1 + D_{26}^* \alpha_2),$$

where

$$\Delta = A_{11}A_{22}A_{66} - A_{11}A_{26}^2 + 2A_{12}A_{16}A_{26} - A_{66}A_{12}^2 - A_{22}A_{16}^2,$$

$$A_{11}^{*}=\frac{A_{22}A_{66}-A_{26}^{2}}{\Delta},A_{12}^{*}=\frac{A_{16}A_{26}-A_{12}A_{66}}{\Delta},A_{16}^{*}=\frac{A_{12}A_{26}-A_{22}A_{16}}{\Delta},$$

$$A_{26}^{*}=\frac{A_{12}A_{16}-A_{11}A_{26}}{\Delta},A_{66}^{*}=\frac{A_{11}A_{22}-A_{12}^{2}}{\Delta},$$

$$\begin{aligned}
&B_{11}^{*}=A_{11}^{*}B_{11}+A_{12}^{*}B_{12}+A_{16}^{*}B_{16},B_{22}^{*}=A_{12}^{*}B_{12}+A_{22}^{*}B_{22}+A_{26}^{*}B_{26},\\
&B_{66}^{*}=A_{16}^{*}B_{16}+A_{26}^{*}B_{26}+A_{66}^{*}B_{66},B_{12}^{*}=A_{11}^{*}B_{12}+A_{12}^{*}B_{22}+A_{16}^{*}B_{26},\\
&B_{21}^{*}=A_{12}^{*}B_{11}+A_{22}^{*}B_{12}+A_{26}^{*}B_{16},B_{16}^{*}=A_{11}^{*}B_{16}+A_{12}^{*}B_{26}+A_{16}^{*}B_{66},\\
&B_{61}^{*}=A_{16}^{*}B_{11}+A_{26}^{*}B_{12}+A_{66}^{*}B_{16},B_{26}^{*}=A_{12}^{*}B_{16}+A_{22}^{*}B_{26}+A_{26}^{*}B_{66},\\
&B_{62}^{*}=A_{16}^{*}B_{12}+A_{26}^{*}B_{22}+A_{66}^{*}B_{26},D_{11}^{*}=A_{11}^{*}A_{11}+A_{12}^{*}A_{12}+A_{16}^{*}A_{16},\\
&D_{22}^{*}=A_{12}^{*}A_{12}+A_{22}^{*}A_{22}+A_{26}^{*}A_{26},D_{12}^{*}=A_{11}^{*}A_{12}+A_{12}^{*}A_{22}+A_{16}^{*}A_{26},\\
&D_{21}^{*}=A_{12}^{*}A_{11}+A_{22}^{*}A_{12}+A_{26}^{*}A_{16},D_{16}^{*}=A_{16}^{*}A_{11}+A_{26}^{*}A_{12}+A_{66}^{*}A_{16},\\
&D_{26}^{*}=A_{16}^{*}A_{12}+A_{26}^{*}A_{22}+A_{66}^{*}A_{26}.
\end{aligned}\tag{20}$$

Substituting once again Eq. (19) into the expression of M_{ij} in Eq. (16b), then M_{ij} into Eq. (18c) leads to:

$$\begin{aligned}
&N_{x,x}+N_{xy,y}=0,\\
&N_{xy,x}+N_{y,y}=0,\\
&P_1f_{,xxxx}+P_2f_{,yyyy}+P_3f_{,xxyy}+P_4f_{,xxxy}+P_5f_{,xyyy}+P_6w_{,xxxx}+P_7w_{,yyyy}+P_8w_{,xxyy}\\
&+P_9w_{,xxxy}+P_{10}w_{,xyyy}+f_{,yy}w_{,xx}-2f_{,xy}w_{,xy}+f_{,xx}w_{,yy}+q-k_1\mathrm{w}+k_2\nabla^2\mathrm{w}+\frac{f_{,xx}}{R}=0,
\end{aligned}\tag{21}$$

in which

$$\begin{aligned}
&P_1=B_{21}^{*},P_2=B_{12}^{*},P_3=B_{11}^{*}+B_{22}^{*}-2B_{66}^{*},\\
&P_4=2B_{26}^{*}-B_{61}^{*},P_5=2B_{16}^{*}-B_{62}^{*},\\
&P_6=B_{11}B_{11}^{*}+B_{12}B_{21}^{*}+B_{16}B_{61}^{*},P_7=B_{12}B_{12}^{*}+B_{22}B_{22}^{*}+B_{26}B_{62}^{*},\\
&P_8=B_{11}B_{12}^{*}+B_{12}B_{22}^{*}+B_{16}B_{62}^{*}+B_{12}B_{11}^{*}+B_{22}B_{21}^{*}+B_{26}B_{61}^{*}\\
&+4B_{16}B_{16}^{*}+4B_{26}B_{26}^{*}+4B_{66}B_{66}^{*},\\
&P_9=2(B_{11}B_{16}^{*}+B_{12}B_{26}^{*}+B_{16}B_{66}^{*}+B_{16}B_{11}^{*}+B_{26}B_{21}^{*}+B_{66}B_{61}^{*}),\\
&P_{10}=2(B_{12}B_{16}^{*}+B_{22}B_{26}^{*}+B_{26}B_{66}^{*}+B_{16}B_{12}^{*}+B_{26}B_{22}^{*}+B_{66}B_{62}^{*}).
\end{aligned}\tag{22}$$

$f(x,y)$ is the stress function defined by:

$$N_x=f_{,yy},\ N_y=f_{,xx},\ N_{xy}=-f_{,xy}.\tag{23}$$

For an imperfect composite panel, Eq. (21) is modified into the following form:

$$\begin{aligned}
&P_1f_{,xxxx}+P_2f_{,yyyy}+P_3f_{,xxyy}+P_4f_{,xxxy}+P_5f_{,xyyy}+P_6w_{,xxxx}+P_7w_{,yyyy}+P_8w_{,xxyy}\\
&+P_9w_{,xxxy}+P_{10}w_{,xyyy}+f_{,yy}w_{,xx}-2f_{,xy}w_{,xy}+f_{,xx}w_{,yy}+q-k_1\mathrm{w}+k_2\nabla^2\mathrm{w}+\frac{f_{,xx}}{R}=0,
\end{aligned}\tag{24}$$

in which $w^*(x,y)$ is a known function representing the initial small imperfection of the panels.

The geometrical compatibility equation for an imperfect composite panel is written as [12]:

$$\varepsilon^0_{x,yy}+\varepsilon^0_{y,xx}-\gamma^0_{xy,xy}=w^2_{,xy}-w_{,xx}w_{,yy}+2w_{,xy}w^*_{,xy}-w_{,xx}w^*_{,yy}-w_{,yy}w^*_{,xx}-\frac{w_{,xx}}{R}. \tag{25}$$

From the constitutive relations in Eq. (19), in conjunction with Eq. (23), one can write:

$$\begin{aligned}
\varepsilon^0_x &= A^*_{11}N_x+A^*_{12}N_y+A^*_{16}N_{xy}-B^*_{11}k_x-B^*_{12}k_y-B^*_{16}k_{xy}+\Delta T(D^*_{11}\alpha_1+D^*_{12}\alpha_2),\\
\varepsilon^0_y &= A^*_{12}N_x+A^*_{22}N_y+A^*_{26}N_{xy}-B^*_{21}k_x-B^*_{22}k_y-B^*_{26}k_{xy}+\Delta T(D^*_{21}\alpha_1+D^*_{22}\alpha_2),\\
\gamma^0_{xy} &= A^*_{16}N_x+A^*_{26}N_y+A^*_{66}N_{xy}-B^*_{61}k_x-B^*_{62}k_y-B^*_{66}k_{xy}+\Delta T(D^*_{16}\alpha_1+D^*_{26}\alpha_2).
\end{aligned} \tag{26}$$

Setting Eq. (26) into Eq. (25) gives the compatibility equation of an imperfect composite panel as:

$$\begin{aligned}
&A^*_{22}f_{,xxxx}+A^*_{11}f_{,yyyy}+E_1f_{,xxyy}-2A^*_{16}f_{,xyyy}-2A^*_{26}f_{,xxxy}\\
&+B^*_{21}w_{,xxxx}+B^*_{12}w_{,yyyy}+E_2w_{,xxyy}+E_3w_{,xxxy}+E_4w_{,xyyy}\\
&-\left(w^2_{,xy}-w_{,xx}w_{,yy}+2w_{,xy}w^*_{,xy}-w_{,xx}w^*_{,yy}-w_{,yy}w^*_{,xx}-\frac{w_{,xx}}{R}\right)=0,
\end{aligned} \tag{27}$$

where

$$E_1=2A^*_{12}+A^*_{66},E_2=B^*_{11}+B^*_{22}-2B^*_{66},E_3=2B^*_{26}-B^*_{61},E_4=2B^*_{16}-B^*_{62}. \tag{28}$$

Eq. (24) and Eq. (27) are nonlinear equations in terms of variables w and f, and

are used to investigate the static stability of thin composite panels in thermal environments.

In the present study, the edges of the composite panels are assumed to be simply supported. Two edges $x=0,a$ are freely movable, whereas the remaining two edges $y=0,b$ are immovable. The boundary conditions are defined as:

$$\begin{aligned}
&w=N_{xy}=\phi_y=M_x=P_x=0,\ N_x=N_{x0}\ \text{at}\ \ x=0,a\\
&w=v=\phi_x=M_y=P_y=0,\ N_y=N_{y0}\ \text{at}\ \ y=0,b
\end{aligned} \tag{29}$$

where N_{x0}, N_{y0} are fictitious compressive edge loads at immovable edges.

The approximate solutions of w, w^* and f satisfying boundary conditions Eq. (29) are assumed as:

$$\left(w,w^*\right)=\left(W,\mu h\right)\sin\lambda_m x\sin\delta_n y, \tag{30a}$$

$$\begin{aligned}
f &= A_1\cos 2\lambda_m x+A_2\cos 2\delta_n y+A_3\sin\lambda_m x\sin\delta_n y+A_4\cos\lambda_m x\cos\delta_n y\\
&+\frac{1}{2}N_{x0}y^2+\frac{1}{2}N_{y0}x^2,
\end{aligned} \tag{30b}$$

in which $\lambda_m=m\pi/a,\ \delta_n=n\pi/b$, W is amplitude of the deflection, and μ is the imperfection parameter. The coefficients A_i $(i=1\div 4)$ are determined by substitution of Eqs. (30a) and (30b) into Eq. (27), as:

$$A_1 = \frac{\delta_n^2}{32\,\mathrm{A}_{22}^* \lambda_m^2}\left(W + 2\mu h\right)W, A_2 = \frac{\lambda_m^2}{32\,\mathrm{A}_{11}^* \delta_n^2}\left(W + 2\mu h\right)W,$$
$$A_3 = \frac{\left(Q_2Q_4 - Q_1Q_3\right)}{Q_2^2 - Q_1^2}W, A_4 = \frac{\left(Q_2Q_3 - Q_1Q_4\right)}{Q_2^2 - Q_1^2}W, \quad (31)$$

with

$$Q_1 = \left(A_{22}^*\lambda_m^4 + A_{11}^*\delta_n^4 + E_1\lambda_m^2\delta_n^2\right), Q_2 = 2\left(A_{16}^*\lambda_m\delta_n^3 + A_{26}^*\lambda_m^3\delta_n\right),$$
$$Q_3 = \left(\frac{\lambda_m^2}{R} - B_{21}^*\lambda_m^4 - B_{12}^*\delta_n^4 - E_2\lambda_m^2\delta_n^2\right), Q_4 = \left(E_3\lambda_m^3\delta_n + E_4\lambda_m\delta_n^3\right). \quad (32)$$

Substitution of Eqs. (30a), and (30b) into Eq. (24) and applying the Galerkin procedure for the resulting equation yields:

$$\begin{aligned}
&\frac{ab}{4}\Bigg[\left(P_1\lambda_m^4 + P_2\delta_n^4 + + P_3\lambda_m^2\delta_n^2 - \frac{\lambda_m^2}{R}\right)\frac{\left(Q_2Q_4 - Q_1Q_3\right)}{Q_2^2 - Q_1^2} \\
&-\left(P_4\lambda_m^3\delta_n + P_5\lambda_m\delta_n^3\right)\frac{\left(Q_2Q_3 - Q_1Q_4\right)}{Q_2^2 - Q_1^2} + P_6\lambda_m^4 + P_7\delta_n^4 + P_8\lambda_m^2\delta_n^2 - k_2\left(\lambda_m^4 + \delta_n^4 + 2\lambda_m^2\delta_n^2\right) - k_1\Bigg]W \\
&+\frac{8}{3}\frac{\left(Q_2Q_4 - Q_1Q_3\right)}{Q_2^2 - Q_1^2}\lambda_m\delta_n W\left(W + \mu h\right) \\
&+\left[\frac{\delta_n}{6RA_{22}^*\lambda_m} - \frac{2\lambda_m\delta_n}{3}\left(\frac{P_1}{A_{22}^*} + \frac{P_2}{A_{11}^*}\right)\right]W\left(W + 2\mu h\right) \\
&-\frac{ab}{64}\left(\frac{\delta_n^4}{A_{22}^*} + \frac{\lambda_m^4}{A_{11}^*}\right)W\left(W + \mu h\right)\left(W + 2\mu h\right) \\
&+\frac{4q}{\lambda_m\delta_n} + \frac{4N_{y0}}{R\lambda_m\delta_n} - \frac{ab}{4}\left(N_{x0}\lambda_m^2 + N_{y0}\delta_n^2\right)\left(W + \mu h\right) = 0,
\end{aligned} \quad (33)$$

where m,n are odd numbers. This is the basic equation governing the nonlinear response of three-phase polymer composite panels under mechanical and thermal loads.

3. Nonlinear stability analysis

3.1. Thermal stability analysis

Consider a simply supported polymer composite panel subjected to temperature environments uniformly raised from the stress-free initial state T_i to the final value T_f, and the temperature increment $\Delta T = T_f - T_i$ is constant. In this case, $q = 0$. Note that there is no load at two edges $y = 0, a$, and we have $N_{yo} = 0$.

The in-plane condition on immovability at $y = 0, b$, i.e. $v = 0$ at $y = 0, b$, is fulfilled in an average sense as:

$$\int_0^a \int_0^b \frac{\partial v}{\partial y} dy dx = 0. \qquad (34)$$

From Eq. (11) and Eq. (19), one can obtain the following expressions in which Eq. (23) and imperfection have been included:

$$\frac{\partial v}{\partial y} = A_{12}^* f_{,yy} + A_{22}^* f_{,xx} - A_{26}^* f_{,xy} + B_{21}^* w_{,xx} + B_{22}^* w_{,yy} + 2B_{26}^* w_{,xy} + \Delta T(D_{21}^* \alpha_1 + D_{22}^* \alpha_2) + \frac{w}{R} - \frac{w_{,y}^2}{2} - w_{,y} w_{,y}^*. \qquad (35)$$

Substitution of Eq. (30a) and Eq. (30b) into Eq. (35), and then the results into Eq. (34) gives fictitious edge compressive loads as:

$$N_{xo} = J_1 W + J_2 W\left(W + 2\mu h\right) + J_3 \Delta T, \qquad (36)$$

with specific expressions of coefficients J_i $(i = \overline{1,3})$ defined in Appendix A.

Subsequently, setting Eq. (36) into Eq. (33) gives:

$$\Delta T = b_1^1 \overline{W} + b_2^1 \frac{\overline{W}}{\left(\overline{W} + \mu\right)} + b_3^1 \frac{\overline{W}\left(\overline{W} + 2\mu\right)}{\left(\overline{W} + \mu\right)} - b_4^1 \overline{W}\left(\overline{W} + 2\mu\right). \qquad (37)$$

in which specific expressions of coefficients b_i^1 $(i = \overline{1,4})$ are given in Appendix A and $\overline{W} = \frac{W}{h}$.

3.2. Thermo-mechanical stability analysis

The simply supported three-phase polymer composite panel with tangentially restrained edges is assumed to be subjected to external pressure q uniformly distributed on the outer surface of the panel and exposed to a uniformly raised temperature field.

Setting Eq. (36) into Eq. (33) gives:

$$q = b_1^{1*} \overline{W} + b_2^{1*} \overline{W}\left(\overline{W} + \mu\right) + b_3^{1*} \overline{W}\left(\overline{W} + 2\mu\right) + b_4^{1*} \overline{W}\left(\overline{W} + \mu\right)\left(\overline{W} + 2\mu\right) + b_5^{1*}\left(\overline{W} + \mu\right)\Delta T. \qquad (38)$$

in which specific expressions of coefficients b_i^{1*} $(i = \overline{1,5})$ are given in Appendix B

4. Numerical results and discussion

We chose the three-phase composite polymer with the properties of the component phase as shown in Table 1.

Table 1. Properties of the component phases for the three-phase composites [11, 12].

Component phase	Young's modulus E	Poisson's ratio ν	Thermal expansion coefficient α
Matrix epoxy	2.75 *GPa*	0.35	54×10^{-6} /^{o} *C*
Glass fibre	22 *GPa*	0.24	5×10^{-6} /^{o} *C*
Titanium oxide TiO_2	5.58 *GPa*	0.2	4×10^{-6} /^{o} *C*

To validate the accuracy of the present method, Fig. 2 compares the results of this paper for symmetric sandwich laminated three-phase polymer composite panels resting on elastic foundations under uniform temperature rise with a stacking sequence of [0/90/0/90/0] and immovable edges, with the results given in the work of Duc and Thu [11]. As can be seen, good agreement is obtained in this comparison.

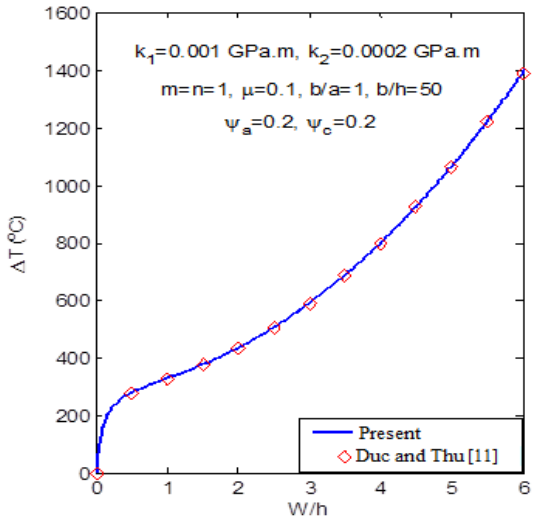

Fig. 2. Comparisons of nonlinear load-deflection curves with the results of Duc and Thu (2014) for the symmetric sandwich laminated three-phase polymer composite panels under uniform temperature rise.

The results presented in this section from Eq. (31) correspond to a deformation mode with half-wave numbers $m = n = 1$.

Scanning electron microscope (SEM) instrumentation at the Laboratory for Micro-Nano Technology, University of Engineering and Technology, Vietnam National University, Hanoi, was used. Figs. 3 and 4 show the SEM images of fabricated samples of composite structures, which were made in the Institute of Ship building, Nha Trang University [12]. Fig. 3 illustrates an SEM image of 2Dm composite polymer two-phase material (glass fibre volume fraction of 25% without particles), and Fig. 4 shows an SEM image of 2Dm composite polymer three-phase material (glass fibre volume fraction of 25% and titanium dioxide particle volume fraction of 3%). Obviously, when the particles are doped, the air cavities significantly reduce and the material was finer. In other words, the particles enhance the stiffness and penetration resistance of the materials.

Next, we will investigate the influences of fibres and particles, material and geometrical properties, foundation stiffness, imperfection, and temperature on the nonlinear response of the three-phase composite panel.

We consider the sandwich five-layer symmetric panel with a stacking sequence of [45/-45/0/-45/45]. The mass density of the panel is $\rho = 1550 kg / m^3$.

Figs. 5 and 6 show the effects of fibres volume fraction ψ_a and particle volume fraction ψ_c on the nonlinear response of the three-phase composite panels under uniform temperature rise and uniform external pressure, respectively. Obviously, the load-carrying capacity of the panel increases when the fibre and the particle volume fractions increase.

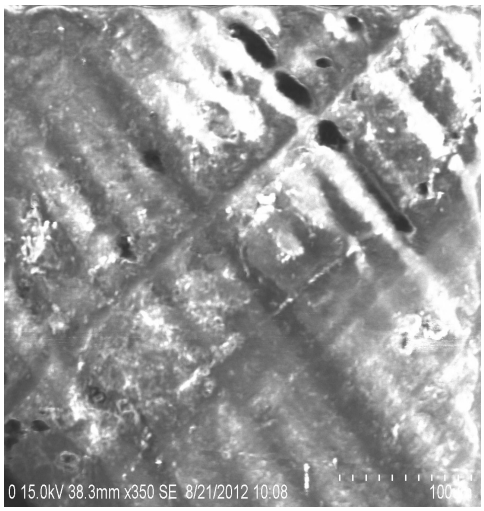

Fig 3. SEM image of 2Dm composite two-phase material (fibre volume fraction is 25% without particles).

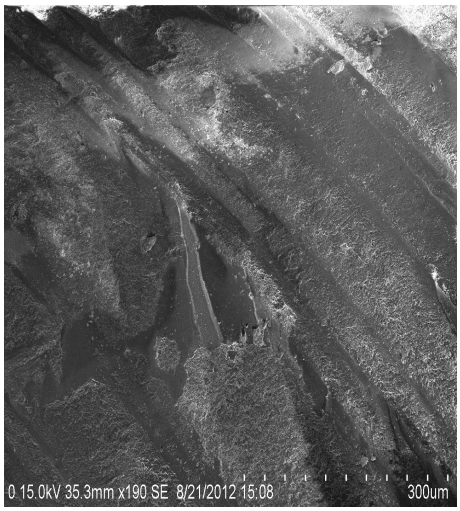

Fig. 4. SEM image of 2Dm composite three-phase material (fibre volume fraction is 25% and particle volume fraction is 3%).

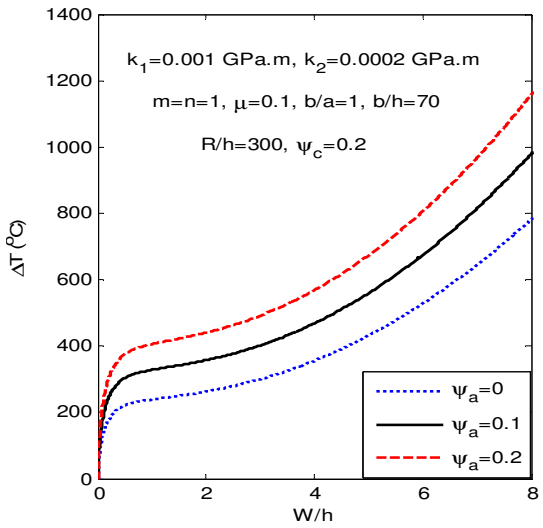

Fig. 5. Effects of fibre volume fraction ψ_a on the nonlinear response of the three-phase nanocomposite panels under uniform temperature rise.

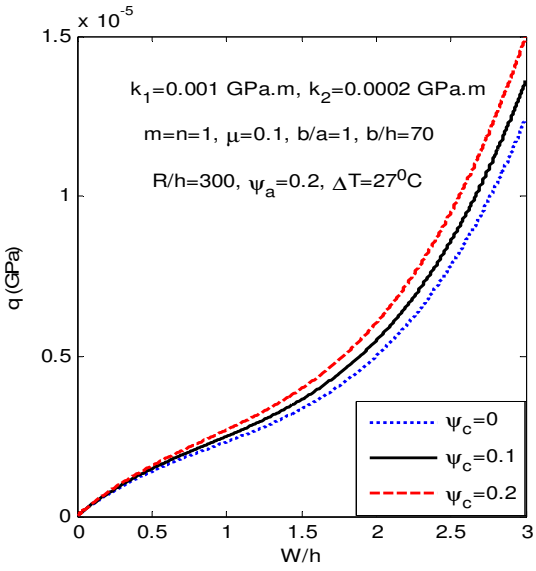

Fig. 6. Effects of particle volume fraction ψ_c on the nonlinear response of the three-phase nanocomposite panels under uniform external pressure.

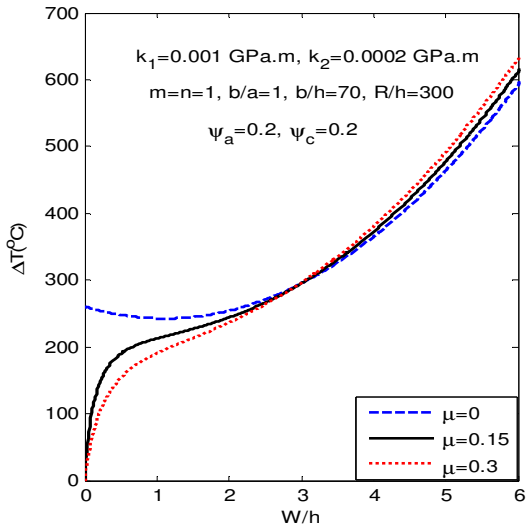

Fig. 7. Effect of imperfection parameter μ on the nonlinear response of the three-phase nanocomposite panels under uniform temperature rise.

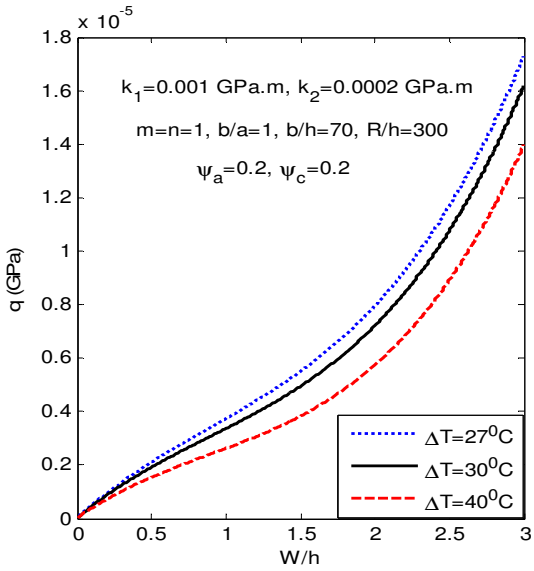

Fig. 8. Effect of temperature increment on the nonlinear stability of the three-phase nanocomposite panels under uniform external pressure.

The effect of initial imperfection with the coefficient μ on the nonlinear response of the three-phase nanocomposite panels under uniform temperature rise is shown in Fig. 7. Three values of $\mu = 0, 0.15, 0.3$ are used. It can be seen that the initial imperfection considerably impacted on the nonlinear response of the three-phase nanocomposite panels.

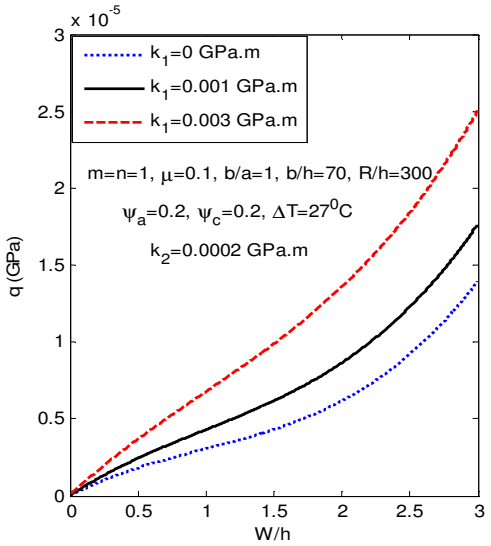

Fig. 9. Effect of the linear Winkler foundation on the nonlinear response of the three-phase nanocomposite panels under uniform external pressure.

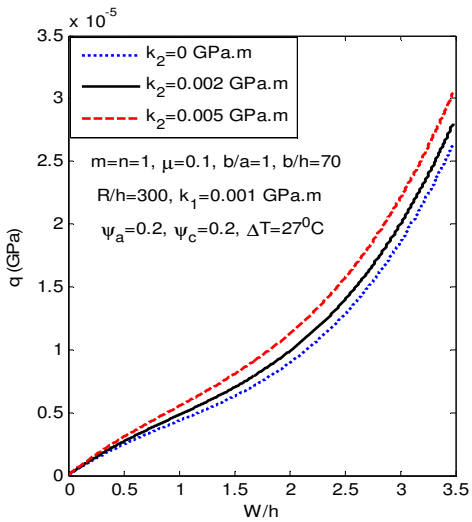

Fig. 10. Effect of the Pasternak foundation on the nonlinear response of the three-phase nanocomposite panels under uniform external pressure.

Fig. 8 indicates the effects of temperature increment ΔT on the post-buckling response of the three-phase nanocomposite panels under uniform external pressure with immovable edges. As can be seen, an increase in temperature increment leads to a reduction of load-carrying capacity of the panels.

Figs. 9 and 10 illustrate the effects of elastic foundations with coefficients k_1 and k_2 on the nonlinear response of three-phase nanocomposite panels under uniform external pressure, respectively. Clearly, the load-carrying capacity of the panel becomes considerably higher due to the support of elastic foundations. Furthermore, the beneficial effect of the Pasternak foundation on the post-buckling response of the three-phase nanocomposite panels is better than of the Winkler one.

Figs. 11 and 12 show the influences of b/a ratio and b/h ratio on the nonlinear postbuckling of three-phase nanocomposite panels under uniform temperature rise and uniform external pressure, respectively. One can see that the load-carrying capacity of the panel increases when the b/a ratio and b/h ratio decrease.

The effect of R/h ratio on the nonlinear response of three-phase nanocomposite panels under uniform external pressure is also presented in Fig. 13. The results from this figure show that the buckling and post-buckling loads are very sensitive to a change of R/h ratio.

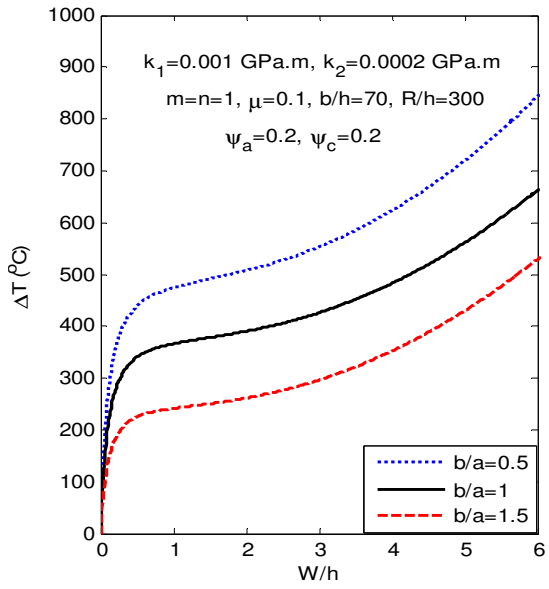

Fig. 11. Effect of b/a ratio on the nonlinear response of three-phase nanocomposite panels under uniform temperature rise.

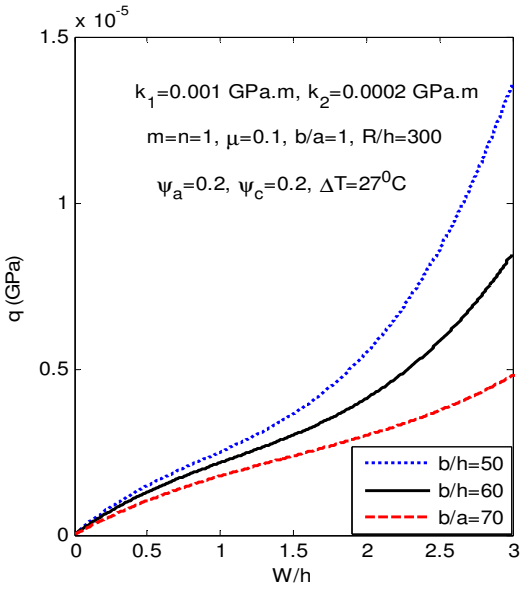

Fig. 12. Effect of b/h ratio on the nonlinear response of three-phase nanocomposite panels under uniform external pressure.

Fig. 14 compares the nonlinear static stability of three-phase sandwich laminated polymer composite panels in two cases: a five-layer asymmetric panel with a stacking sequence of [0/45/45/-45/-45]; and a five-layer symmetric panel with a stacking sequence of [45/-45/0/-45/45]. This comparison is performed on panels with the same ply orientations and the same thickness. The result shows that the load-carrying capacity of a symmetric panel is higher than that of an asymmetric panel.

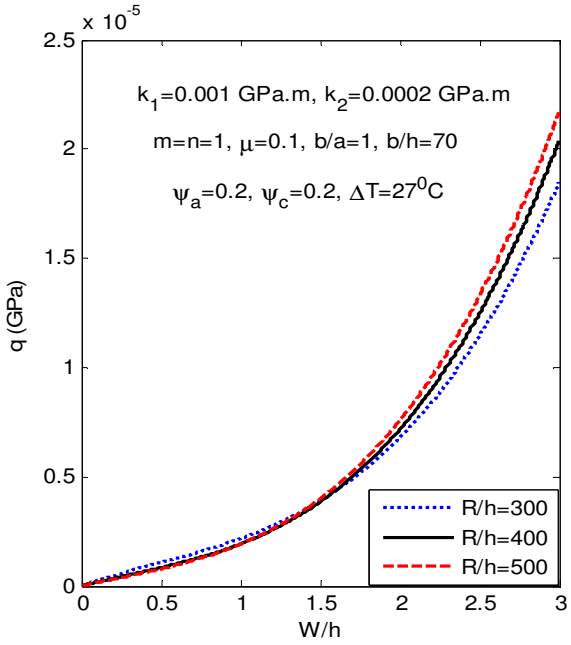

Fig. 13. Effect of R/h ratio on the nonlinear response of three-phase nanocomposite panels under uniform external pressure.

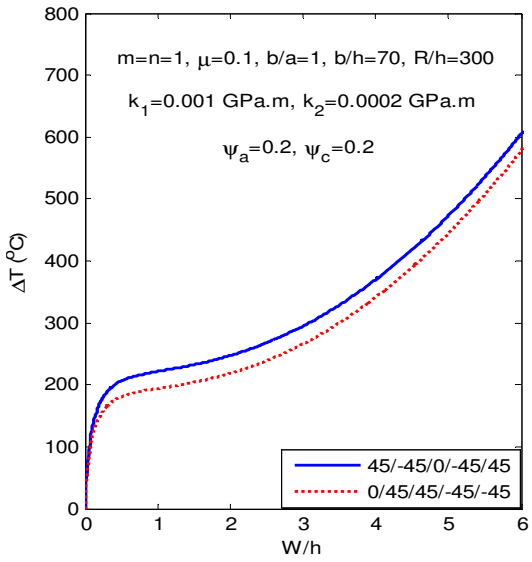

Fig. 14. Effects of fibre angles on the nonlinear response of symmetric and asymmetric three-phase nanocomposite panels under uniform temperature rise.

5. Conclusions

Based on classical shell theory, this paper investigated the nonlinear stability analysis of imperfect sandwich laminated three-phase polymer nanocomposite panels resting on elastic foundations in thermal environments.

From the numerical results, the following conclusions are made:

- Increasing the density of fibres and particles in three-phase composite polymers improves the mechanical and thermal loading ability of the composite panels. However, the effects of the fibres are stronger than those of the particles.

- With the same thickness and size, the thermal loading ability of the symmetric panel is better than that of the asymmetric panel.

- The elastic foundations have a strong effect on the nonlinear response of the three-phase composite panels; and the beneficial effect of the Pasternak foundation is better than the Winkler one.

- The geometry, initial imperfection, and temperature have a significant effect on the stability of the composite panel.

Acknowledgement

This work was supported by the Grant of Newton Fund Code NRCP1516/1/68. The authors are grateful for this support.

References

[1] Díaz RG, Ramos RR, Castillero JB, Sabina FJ. Montes HC. Electro-mechanical moduli of three-phase fiber composites. Mater Let 2008;62(16):2385-2387.

[2] Duc ND, Minh DK. Bending analysis of three-phase polymer composite plates reinforced by glass fibers and titanium oxide particles. J Comput Mater Sci 2010;49(4):S194-198.

[3] Lee JH, Rhee KY, Park SJ. Silane modification of carbon nanotubes and its effects on the material properties of carbon/CNT/epoxy three-phase composites. Compos Part A Appl Sci Manu 2011;42(5):478-483.

[4] Hoh HJ, Xiao ZM, Luo J. Crack tip opening displacement of a Dugdale crack in a three-phase cylindrical model composite material. Int J Eng Sci 2011;49(6):523-535.

[5] Wu J, Liu J, Yang F. Three-phase composite conductive concrete for pavement deicing. Construct Build Mater 2015;75:129-135.

[6] Wang X, Zhou K. Three-phase elliptical inclusions with internal uniform hydrostatic stress resultants in isotropic laminated plates. Euro J Mech A Solids 2015;49:125-36.

[7] Chung DN, Dinh NN, Hui D, Duc ND, Trung NQ, Chipara M. Investigation of polymeric composite films using modified TiO_2 nanoparticles for organic light emitting diodes. J Cur Nanosci 2013;9(1):14-20.

[8] Kalamkarov AL, Andrianov IV, Starushenko GA. Three-phase model for a composite material with cylindrical circular inclusions. Part I: Application of the boundary shape perturbation method. Int J Eng Sci 2014;78:154-177.

[9] Zhang Z, Gu Y, Wang S, Li M, Bi J, Zhang Z. Enhancement of dielectric and electrical properties in BT/SiC/PVDF three-phase composite through microstructure tailoring. Compos Part A Appl Sci Manu 2015;74:88-95.

[10] Chen L, Li P, Wen Y, Zhu Y. Large self-biased effect and dual-peak magnetoelectric effect in different three-phase magnetostrictive/piezoelectric composites. J Alloy Comp 2014;606:15-20.

[11] Duc ND, Thu PV. Nonlinear stability analysis of imperfect three-phase polymer composite plates in thermal environments. Compos Struct 2014;109:130-138.

[12] Duc ND, Homayoun H, Thu PV, Quan TQ. Vibration and nonlinear dynamic response of imperfect three-phase polymer nanocomposite panel resting on elastic foundations under hydrodynamic loads. Compos Struct 2015;131:229-237.

[13] Hu HS, Nie JG, Eatherton MR. Deformation capacity of concrete-filled steel plate composite shear walls. J Construct Steel Research 2014;103:148-158.

[14] Song Y, Feng L, Wen J, Yu D, Wen X. Reduction of the sound transmission of a periodic sandwich plate using the stop band concept. Compos Struct 2015;128:428-436.

[15] Mauritsson K, Folkow PD. Dynamic equations for a fully anisotropic piezoelectric rectangular plate. Comput Struct 2015;153:112-125.

[16] Bochkarev SA, Lekomtsev SV, Matveenko VP. Parametric investigation of the stability of coaxial cylindrical shells containing flowing fluid. Euro J Mech A Solids 2014;47:174-181.

[17] Joshi PV, Jain NK, Ramtekkar GD. Effect of thermal environment on free vibration of cracked rectangular plate: An analytical approach. Thin Wall Struct 2015;91:38-49.

[18] Kang P, Youn SK. Isogeometric analysis of topologically complex shell structures. Finite Elem Anal Des 2015;99:68-81.

[19] Jam JE, Kiani Y. Buckling of pressurized functionally graded carbon nanotube reinforced conical shells. Compos. Struct. 2015;125:586-595.

[20] Wali M, Hentati T, Jarraya A, Dammak F. Free vibration analysis of FGM shell structures with a discrete double directors shell element. Compos. Struct. 2015;125:295-303.

[21] Li X, Yu K, Han J, Zhao R, Wu Y. A piecewise shear deformation theory for free vibration of composite and sandwich panels. Compos Struct 2015;124:111-119.

[22] Duc ND, Tung HV, Hang DT. An alternative method determining the coefficient of thermal expansion of composite material of spherical particles. Vietnam J Mech, VAST 2007;29(1):58-64.

[23] Vanin GA. Micro-Mechanics of composite materials, Nauka Dumka, Kiev, 1985.

[24] Kamarian S, Sadighi M, Shakeri M, Yas MH. Free vibration response of sandwich cylindrical shells with functionally graded materials face sheets resting on Pasternak foundation. Journal of Sandwich Structures and Materials 2014; 16: 511-533.

Appendix A

$$J_1=\left\{\begin{array}{l}\dfrac{4n\left(A_{12}^*A_{12}^*-A_{22}^*A_{11}^*\right)\left(Q_2Q_4-Q_1Q_3\right)}{b^2m\left(Q_2^2-Q_1^2\right)\left[A_{12}^{*\,2}-A_{11}^*A_{22}^*\right]}+\dfrac{4\left(A_{12}^*A_{26}^*-A_{22}^*A_{16}^*\right)\left(Q_2Q_3-Q_1Q_4\right)}{ab\left(Q_2^2-Q_1^2\right)\left[A_{12}^{*\,2}-A_{11}^*A_{22}^*\right]}\\ +\dfrac{4m\left(A_{12}^*B_{21}^*-A_{22}^*B_{11}^*\right)}{a^2n\left[A_{12}^{*\,2}-A_{11}^*A_{22}^*\right]}+\dfrac{4n\left(A_{12}^*B_{22}^*-A_{22}^*B_{12}^*\right)}{b^2m\left[A_{12}^{*\,2}-A_{11}^*A_{22}^*\right]}-\dfrac{4A_{12}^*}{Rmn\pi^2\left[A_{12}^{*\,2}-A_{11}^*A_{22}^*\right]}\end{array}\right\},$$

$$J_2=\frac{\left(A_{12}^*\delta_n^2-A_{22}^*\lambda_m^2\right)}{8\left[A_{12}^{*\,2}-A_{11}^*A_{22}^*\right]},\quad J_3=\frac{\left[A_{22}^*(D_{11}^*\alpha_1+D_{12}^*\alpha_2)-A_{12}^*(D_{21}^*\alpha_1+D_{22}^*\alpha_2)\right]}{\left[A_{12}^{*\,2}-A_{11}^*A_{22}^*\right]},$$

$$b_1^1=\frac{32hn\left(Q_2Q_4-Q_1Q_3\right)}{3J_3b^2m\left(Q_2^2-Q_1^2\right)}-\frac{hJ_1}{J_3},$$

$$b_2^1=\frac{1}{J_3}\left(\begin{array}{l}\left[P_1\dfrac{m^2\pi^2}{a^2}+P_2\dfrac{a^2n^4\pi^2}{b^4m^2}+P_3\dfrac{n^2\pi^2}{b^2}-\dfrac{1}{R}\right]\dfrac{\left(Q_2Q_4-Q_1Q_3\right)}{Q_2^2-Q_1^2}\\ -\left[P_4\dfrac{mn\pi^2}{ab}+P_5\dfrac{an^3\pi^2}{b^3m}\right]\dfrac{\left(Q_2Q_3-Q_1Q_4\right)}{Q_2^2-Q_1^2}\\ +P_6\dfrac{m^2\pi^2}{a^2}+P_7\dfrac{a^2n^4\pi^2}{b^4m^2}+P_8\dfrac{n^2\pi^2}{b^2}-k_2\left(1+\dfrac{a^2n^2}{b^2m^2}\right)-\dfrac{k_1a^2}{m^2\pi^2}\end{array}\right),$$

$$b_3^1=\frac{2a^2n}{3hJ_3RA_{22}^*b^2m^3\pi^2}-\frac{8n}{3hJ_3b^2m}\left(\frac{P_1}{A_{22}^*}+\frac{P_2}{A_{11}^*}\right),\quad b_4^1=\frac{a^2h^2n^4\pi^2}{16J_3A_{22}^*b^4m^2}+\frac{h^2m^2\pi^2}{16J_3a^2A_{11}^*}+\frac{h^2J_2}{J_3}.$$

Appendix B

$$b_1^{1*}=\left(\begin{array}{l}-\dfrac{h}{16}\left[P_1\dfrac{m^5n\pi^6}{a^4}+P_2\dfrac{mn^5\pi^6}{b^4}+P_3\dfrac{m^3n^3\pi^6}{a^2b^2}-\dfrac{m^3n\pi^4}{a^2R}\right]\dfrac{\left(Q_2Q_4-Q_1Q_3\right)}{Q_2^2-Q_1^2}\\ +\dfrac{h}{16}\left[P_4\dfrac{m^4n^2\pi^6}{a^3b}+P_5\dfrac{m^2n^4\pi^6}{ab^3}\right]\dfrac{\left(Q_2Q_3-Q_1Q_4\right)}{Q_2^2-Q_1^2}-\dfrac{P_6hm^5n\pi^6}{16a^4}\\ -\dfrac{P_7hmn^5\pi^6}{16b^4}-\dfrac{P_8hm^3n^3\pi^6}{16a^2b^2}+\dfrac{hk_2}{16}\left(\dfrac{m^3n\pi^4}{a^2}+\dfrac{mn^3\pi^4}{b^2}\right)+\dfrac{hk_1mn\pi^2}{16}\end{array}\right),$$

$$b_2^{1*}=\frac{J_1h^2m^3n\pi^4}{16a^2}-\frac{2h^2m^2n^2\pi^4\left(Q_2Q_4-Q_1Q_3\right)}{3a^2b^2\left(Q_2^2-Q_1^2\right)},\ b_3^{1*}=\frac{h^2m^2n^2\pi^4}{6a^2b^2}\left(\frac{P_1}{A_{22}^*}+\frac{P_2}{A_{11}^*}\right)-\frac{h^2n^2\pi^2}{24A_{22}^*b^2R},$$

$$b_4^{1*}=\left\{\frac{h^3}{256}\left(\frac{mn^5\pi^6}{A_{22}^*b^4}+\frac{m^5n\pi^6}{A_{11}^*a^4}\right)+\frac{J_2h^3m^3n\pi^4}{16a^2}\right\},\ b_5^{1*}=\frac{hm^3n\pi^3}{16a^2}.$$